The 8th European Congress on Computational Methods in Applied Sciences and Engineering
ECCOMAS Congress 2022
5-–9 June 2022, Oslo, Norway

TAUT DOMAIN ANALYSIS OF TRANSVERSELY ISOTROPIC DIELECTRIC ELASTOMER MEMBRANES

Aman Khurana[1], Giuseppe Zurlo[2], and M. M. Joglekar[1*]

[1] Department of Mechanical and Industrial Engineering
Indian Institute of Technology Roorkee 247667, India
e-mail: manish.joglekar@me.iitr.ac.in

[2] Stokes Centre of Applied Mathematics, School of Mathematics,
Statistics and Applied Mathematics, NUI Galway, University Road, Galway, Ireland

Key words: Dielectric elastomers, Wrinkling, Taut domain, Anisotropy, Fiber orientations, Electroelasticity

Abstract. Actuation devices made of dielectric elastomers are prone to compression induced wrinkling instabilities, which can adversely affect their performance and may lead to device failure. On the other hand, wrinkles can be used constructively in certain applications demanding a controlled alternation of the surface morphology. The idea of taut states and the natural width under simple tension plays an important role in the analysis of compression generated instability (wrinkling). In case of electrically driven DE membranes, the domain of taut states in the plane of principal stretches is influenced substantially by the applied voltage and the film's constitutive properties. In the recent past, there has been an increasing interest in exploiting anisotropy in the material behavior of dielectric elastomers for improving their actuation performance. Spurred with these ongoing efforts, this paper presents a continuum mechanics based electromechanical model for predicting the thresholds on the domain of taut states of transversely isotropic planar dielectric elastomers. The developed analytical framework uses an amended energy function that accounts for the electromechanical coupling for a class of incompressible transversely isotropic dielectric membranes. The required expressions for the total Cauchy stress tensor and the associated principal stress components are evaluated utilizing the amended energy function. Finally, the concept of natural width under simple tension is implemented to obtained the nonlinear coupled electromechanical equation that evaluates the associated taut states domain of the transversely isotropic planar dielectric elastomers.

Our results indicate that the extent of taut domain can be controlled by modifying the level and the principal direction of the transverse isotropy. The taut states domain for a particular level of applied electric field increases with increase in the anisotropy parameter, while the taut domains depleted with the increase in fiber orientations from 0^0 to 90^0 for an applied level of electrical loading. The fiber-reinforced wrinkle-tunable surfaces can be effectively designed and developed using the underlying analytical framework and the trends obtained in this study.

1 INTRODUCTION

Electroactive polymers (EAPs), also known as smart polymers, have attracted considerable interest recently because they can provide smart and innovative solutions for new generation

robot designs and other actuating devices. Electroactive polymers open an exciting field of engineering called soft robotics that emerges the uses of soft smart active materials to create soft machines having multiple input controls like electrical and mechanical [1]. The key motive of having such multiple controlling modes in a single device lies in attaining a quicker and more precise actuator control with high load-carrying capability from the same device. Also, multiple input controls will be the essential need for upcoming intelligent systems used in modern applications like prosthetic limbs [2], minimum energy structures [3, 4], actuators [5], etc .

Most of the engineering materials exhibit nonlinearities due to their inherent properties [6, 7, 8, 9]. Generally, the electroactive polymer actuators also possess material-based nonlinearities [10, 11, 12, 13, 14]. The actuators made of EAPs are typically constituted by a thin polymer sheet sandwiched between two compliant electrodes with an applied electric field source. A suitable electromechanical field source arrangement imposes an electromechanical force on such a smart actuator causes the deformation used as a means of actuation. In such EAPs-based actuator devices, the failure mechanisms are generally determined by a sudden loss of equilibrium due to in-plane compression. The onset of electro-mechanical instability-based deformation localizations has been analyzed in a series of articles [15, 16] and references therein. In this perspective, pre-stretching provides an experimental-based solution to suppress such instability-based failure mechanisms [31]. In EAPs material-based smart polymers, the taut states are simply the in-plane principal stretch conditions for different thin membrane configurations obtained in the activated mode. However, the bending stiffness of the smart membranes is neglected, which results in a compression-induced film buckling of thin membrane [17]. The taut states are typically defined as the region where both in-plane principal stretches are positive (tensile configurations) or a domain where a single principal stretch is positive (wrinkled configurations). At the same time, the remaining region where none principal stretch is positive typically defined as the bounded or balanced region at which a sudden loss of equilibrium condition is not observed like in taut domains, and in such regions, no taut states are possible. In general, the determination of such taut domains plays a significant role in obtaining the critical states of EAPs material-based actuator designs.

To mention some earlier works on the taut domains, various researchers [17, 18, 19] studied the different failure mechanisms related to applied electric field-induced wrinkling phenomenon commonly focusing on the dielectric elastomeric-based actuator designs. Additionally, elastomer-based actuators are subjected to a number of operating instabilities, including pull-in instability [20], dynamic snap-through instability [21], pinnacle vibration [22], and many others, all of which limit their actuation capabilities. To outmaneuver these issues, researchers have used a variety of strategies in the past [4, 23, 30]. Incorporating anisotropy into the material behavior of the elastomeric membrane is one such promising technique [4, 23]. Inspired from such previously reported studies, we herein aim to explore the concept of taut domains in transversely isotropic electroactive thin membranes used explicitly in a new kind of fiber-based smart actuator designs for modern applications. To the best of our knowledge, the current study is motivated to present the taut domains in the fiber-based smart thin membranes for the first time.

The current research is further structured as follows: In Section 2, an electromechanical model based on continuum mechanics is built to predict the thresholds on the taut domains of a transversely isotropic membrane in the plane of principal stretches using the concept of natural width under simple tension. Section 3 presents a comprehensive parametric investigation that

reveals the impact of fibre strength and orientation on the taut domains of a transversely isotropic smart thin membrane under electrical loading. Finally, Section 4 summarises the study's main conclusions and future prospects.

2 Electromechanical model for taut domains in transversely isotropic smart thin membrane

In this section, governing equations pertaining to a transversely isotropic thin membrane under electromechanical loading are presented following the nonlinear electroelasticity theory developed in [24]. Additionally, the central idea of natural width in the context of a tension field theory of thin membranes [25] is introduced for a transversely isotropic electroelastic material class. Furthermore, the nonlinear expressions of taut domains in the transversely isotropic thin membrane are derived.

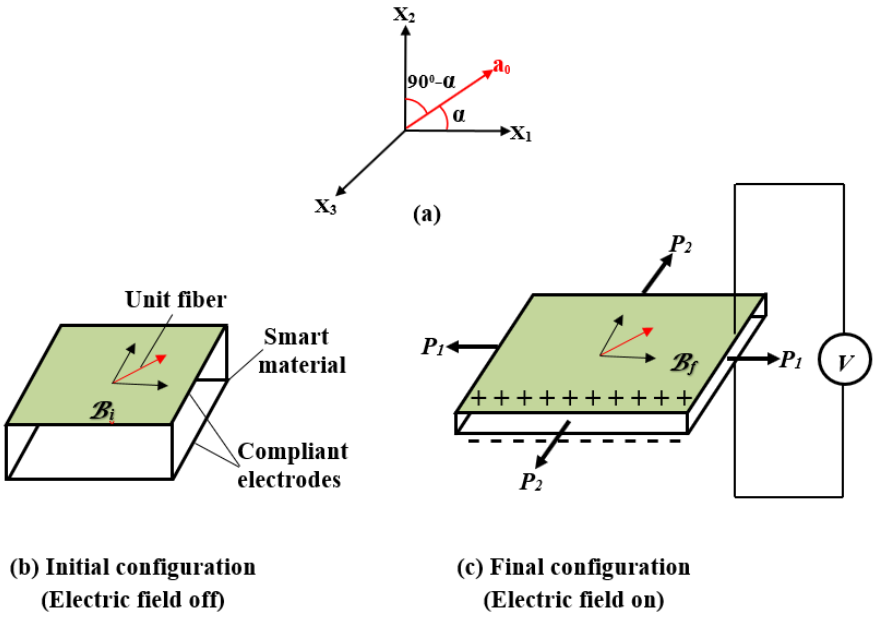

Figure 1: Schematic representations of (a) unit fiber vector orientation in 3D space, (b) undeformed configuration of a smart membrane, and (c) deformed configuration of a smart membrane with electric field loading.

2.1 Governing equation for transversely isotropic smart thin membrane

Consider a transversely isotropic electroelastic membrane in the reference configuration $\mathcal{B}_i$ as shown in Fig.1. The membrane deforms with an applied electrical field in the current configuration $\mathcal{B}_f$ carrying a deformation $\mathbf{f} : \mathcal{B}_i \to \mathcal{B}_f$ with the deformation gradient $\mathbf{F} = \nabla \mathbf{f}$. The left Cauchy–Green deformation tensor $\mathbf{B}$ for the given deformation $\mathbf{f}$ is denoted by $\mathbf{B} = \mathbf{F}\mathbf{F}^T = \sum_{i=1}^{3} \lambda_i^2 \mathbf{e}_i \otimes \mathbf{e}_i$, where λ_i is the i^{th} principal stretch. In the current configuration, the electrical field variables is denoted by $\mathbf{E}$. The fiber-reinforcement in the body is incorporated through

a fiber-vector $\mathbf{a}_0$ in a particular direction (say α) in the reference configuration that has been transformed to $\mathbf{a} = \mathbf{F}\mathbf{a}_0$ with an applied deformation $\mathbf{f}$.

Further, a complete set of invariants for an incompressible transversely isotropic electroelastic material class are introduced by [24]

$$\begin{aligned} I_1 = \mathrm{tr}\mathbf{B} = \lambda_1^2 + \lambda_2^2 + \lambda_1^{-2}\lambda_2^{-2}, \quad I_2 = \frac{1}{2}[(\mathrm{tr}\mathbf{B})^2 - \mathrm{tr}(\mathbf{B}^2)] = \lambda_1^{-2} + \lambda_2^{-2} + \lambda_1^2\lambda_2^2, \\ I_3 = \det\mathbf{B} = \lambda_1\lambda_2\lambda_3 = 1, \quad I_4 = [\mathbf{E}^l \otimes \mathbf{E}^l] : \mathbf{I} = \lambda_3^2 E_0^2, \quad I_5 = [\mathbf{E}^l \otimes \mathbf{E}^l] : \mathbf{B}^{-1} = E_0^2, \\ I_6 = [\mathbf{E}^l \otimes \mathbf{E}^l] : \mathbf{B}^{-2} = \lambda_3^{-2} E_0^2, \quad I_{10} = \mathbf{a_0}.\mathbf{B}\mathbf{a_0} = \lambda_1^2 \mathrm{Cos}^2\alpha + \lambda_2^2 \mathrm{Sin}^2\alpha, \end{aligned} \tag{1}$$

where $\mathbf{E}^l = \mathbf{F}^T\mathbf{E}$ is the electric field vectors defined in Lagrangian form. Now, we write the free energy density for a transversely isotropic electroelastic membrane as $\Omega = \Omega(\mathbf{F}, \mathbf{E}^l, \mathbf{H}^l, \mathbf{a}_0) = \Omega(I_1, I_2, I_3, I_4, I_5, I_6, I_7$. Following the coupled nonlinear theory of electroelasticity [26], an expression of the total stress tensor $\mathbf{T}$ for an incompressible transversely isotropic electro-magneto-elastic material class $\Omega = \Omega(I_1, I_2, I_4, I_5, I_6, I_7)$ is given by

$$\begin{aligned} \mathbf{T} = -p\mathbf{I} + 2\Omega_1\mathbf{B} + 2\Omega_2[I_1\mathbf{B} - \mathbf{B}^2] - 2\Omega_5[\mathbf{E}\otimes\mathbf{E}] - 2\Omega_6[\mathbf{B}^{-1}\mathbf{E}\otimes\mathbf{E} + \mathbf{E}\otimes\mathbf{B}^{-1}\mathbf{E}] \\ +2\Omega_7[\mathbf{a}\otimes\mathbf{a}]], \end{aligned} \tag{2}$$

where p is a Lagrange multiplier associated with the incompressibility constraint and Ω_i is denoted by $\Omega_i = \dfrac{\partial\Omega}{\partial I_i}$, $i = 1, 2, 3....7$. For a given membrane configuration as shown in Fig.1, the deformation gradient tensor $\mathbf{F}$, the left Cauchy–Green deformation tensor $\mathbf{B}$, the electric field vector $\mathbf{E}$, and fiber vector $\mathbf{a}_0$ are defined as

$$\begin{aligned} \mathbf{F} = \lambda_1\mathbf{e}_1\otimes\mathbf{E}_1 + \lambda_2\mathbf{e}_2\otimes\mathbf{E}_2 + \lambda_1^{-1}\lambda_2^{-1}\mathbf{e}_3\otimes\mathbf{E}_3, \quad \mathbf{B} = \mathbf{F}\mathbf{F}^T, \quad \mathbf{E} = E_0\mathbf{e}_3, \\ \mathbf{a}_0 = \mathrm{Cos}\alpha\ \mathbf{e}_1 + \mathrm{Sin}\alpha\ \mathbf{e}_2, \end{aligned} \tag{3}$$

where $\mathbf{E}_1$, $\mathbf{E}_2$, $\mathbf{E}_3$ represent the basis in the undeformed configuration, and $\mathbf{e}_1$, $\mathbf{e}_2$, $\mathbf{e}_3$ are the basis in the deformed configuration. In the current problem, the defined free energy density Ω is specialized to the following neo-Hookean type of material model, which exhibits the snap-through response of the membrane. The corresponding free energy density expression is given by

$$\Omega = \frac{\mu}{2}\left[I_1 - 3\right] - \frac{\varepsilon_0}{2}\left[C_1 I_4 + C_2 I_5\right] + \frac{\mu}{2}\left[\zeta_1\left(I_7 - 1\right)^2\right], \tag{4}$$

where μ, C_1, C_2 are the material constants, ε_0 represent the electrical permittivity, and ζ_1 denote the fiber-reinforcement parameters. Upon invoking the above defined expressions (3) and (4) alongwith the invariant definitions (1) in (2), the principal stress components for the deformed configuration of membrane are obtained as

$$\begin{aligned} T_{11} = -p + \mu\lambda_1^2 + 2\mu\zeta_1\left(\lambda_1^2\mathrm{Cos}^2\alpha + \lambda_2^2\mathrm{Sin}^2\alpha - 1\right)\lambda_1^2\mathrm{Cos}^2\alpha, \\ T_{22} = -p + \mu\lambda_2^2 + 2\mu\zeta_1\left(\lambda_1^2\mathrm{Cos}^2\alpha + \lambda_2^2\mathrm{Sin}^2\alpha - 1\right)\lambda_2^2\mathrm{Sin}^2\alpha, \\ T_{33} = -p + \mu\lambda_1^{-2}\lambda_2^{-2} + C_2\varepsilon_0 E_0^2. \end{aligned} \tag{5}$$

In the above relations (5), the boundary condition of stress-free state, i.e., $T_{33} = 0$ gives the required expression for a Lagrange multiplier that is an indeterminate hydrostatic pressure p as

$$T_{33} = 0 \Rightarrow p = \mu\lambda_1^{-2}\lambda_2^{-2} + C_2\varepsilon_0 E_0^2. \tag{6}$$

Substituting the above expression of Lagrange multiplier p, the required expressions for the principal stress components (T_{11} and T_{22}) are obtained as

$$\begin{aligned} T_{11} &= \mu(\lambda_1^2 - \lambda_1^{-2}\lambda_2^{-2}) - C_2\varepsilon_0 E_0^2 + 2\mu\zeta_1\left(\lambda_1^2\mathrm{Cos}^2\alpha + \lambda_2^2\mathrm{Sin}^2\alpha - 1\right)\lambda_1^2\mathrm{Cos}^2\alpha, \\ T_{22} &= \mu(\lambda_2^2 - \lambda_1^{-2}\lambda_2^{-2}) - C_2\varepsilon_0 E_0^2 + 2\mu\zeta_1\left(\lambda_1^2\mathrm{Cos}^2\alpha + \lambda_2^2\mathrm{Sin}^2\alpha - 1\right)\lambda_2^2\mathrm{Sin}^2\alpha. \end{aligned} \tag{7}$$

For the sake of convenience, the following non-dimensional electric field variable may be introduced in the above governing equations (7), which are defined as

$$e^* = \hat{E}\sqrt{\frac{C_2\varepsilon_0}{\mu}}, \tag{8}$$

where $\hat{E} = E_0/\lambda_1\lambda_2$ represent the nominal electric field. Upon invoking the above defined non-dimensional electric field variable (8) in the governing equations (7), the normalized principal stress components (T_{11}^* and T_{22}^*) are obtained as

$$\begin{aligned} T_{11}^* &= (\lambda_1^2 - \lambda_1^{-2}\lambda_2^{-2}) - e^{*2}\lambda_1^2\lambda_2^2 + 2\zeta_1\left(\lambda_1^2\mathrm{Cos}^2\alpha + \lambda_2^2\mathrm{Sin}^2\alpha - 1\right)\lambda_1^2\mathrm{Cos}^2\alpha, \\ T_{22}^* &= (\lambda_2^2 - \lambda_1^{-2}\lambda_2^{-2}) - e^{*2}\lambda_1^2\lambda_2^2 + h^{*2}\lambda_1^{-2}\lambda_2^{-2} + 2\zeta_1\left(\lambda_1^2\mathrm{Cos}^2\alpha + \lambda_2^2\mathrm{Sin}^2\alpha - 1\right)\lambda_2^2\mathrm{Sin}^2\alpha. \end{aligned} \tag{9}$$

Finally, the first Piola–Kirchhoff (PK-1) stress components S_{ii}^* from the above developed principal stress components (9) may be obtained based on the following conversion given by

$$S_{ii}^*(\lambda_1, \lambda_2, e^*, \xi_1, \alpha) = \mathrm{T}_{\mathrm{ii}}^*(\lambda_1, \lambda_2, \mathrm{e}^*, \xi_1, \alpha)\lambda_{\mathrm{i}}^{-1} \quad \mathrm{i} = 1, 2. \tag{10}$$

2.2 Taut domains in transversely isotropic smart thin membrane

This subsection introduces a concept of the tensile stretches region that is also known as taut domain [25] shown in Fig.2 for a transversely isotropic electroelastic material class. Reconsider a smart thin membrane sheet bonded with two compliant electrodes and an applied electric field source shown in the previous Fig.1. In the reference configuration $\mathcal{B}_i$, the thin membrane is assumed as having a constant thickness with a right cylindrical region in flat mid-surface. At the same time, orthogonal displacements of flat mid-surface are neglected because the membrane remains flat during loading activation.

In order to deduce the constitutive relations for the taut domains a state of local uniaxial stress in direction $\mathbf{e}_2$ is considered. Consequently for uniaxial stress ($T_{11}^* = T_{33}^* = 0$), the transverse stretch in direction $\mathbf{e}_1$ assumes a specific value referred as natural width in tension. Thus, the governing equation (9) for the taut domains of transversely isotropic electroactive thin membrane is rewritten as

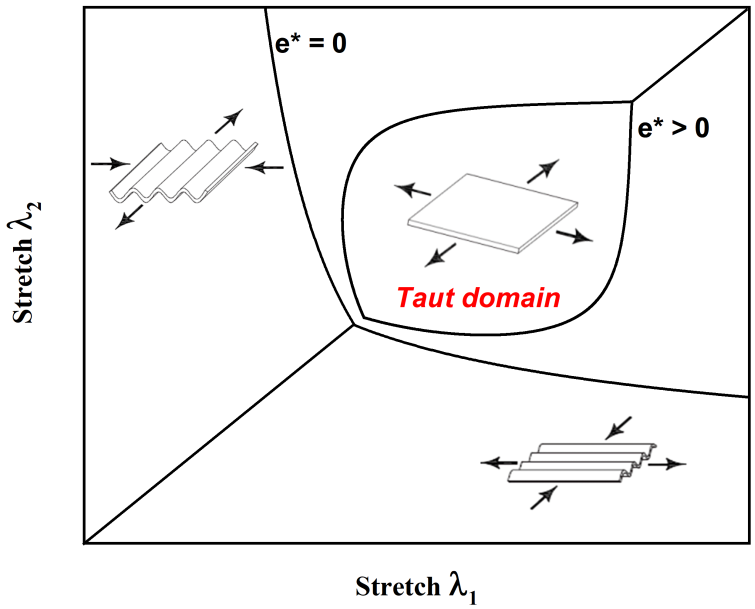

Figure 2: A schematic representation of the natural strain curves of the tensile stretch region.

$$(\lambda_1^2 - \lambda_1^{-2}\lambda_2^{-2}) - e^{*2}\lambda_1^2\lambda_2^2 + 2\zeta_1\left(\lambda_1^2\mathrm{Cos}^2\alpha + \lambda_2^2\mathrm{Sin}^2\alpha - 1\right)\lambda_1^2\mathrm{Cos}^2\alpha. \tag{11}$$

In case of simple boundary value problem, the smart thin membrane is considered with the null tractions on the entire boundary triggered on the upper and lower faces by an applied electric field. Invoking the notion of equibiaxial equilibrium configurations, i.e., $P_1 = P_2 = P$ and $\lambda_1 = \lambda_2 = \lambda$, the Piola–Kirchhoff stress components utilizing (10), are obtained as

$$\begin{aligned} S_{11}^*(\lambda, e^*, \xi_1, \alpha) &= \mathrm{S}_{22}^*(\lambda, e^*, \xi_1, \alpha) = \mathrm{S}^*(\lambda, \mathrm{e}^*, \xi_1, \alpha), \\ \Rightarrow (\lambda - \lambda^{-5}) - e^{*2}\lambda^3 &+ 2\zeta_1\left(\lambda^2\mathrm{Cos}^2\alpha + \lambda^2\mathrm{Sin}^2\alpha - 1\right)\lambda\mathrm{Cos}^2\alpha. \end{aligned} \tag{12}$$

Further, the equibiaxial stretch λ satisfies the conditions of null tractions on the edges of the membrane and corresponds to the following obtained solution

$$\mathrm{S}^*(\lambda, \mathrm{e}^*, \xi_1, \alpha) = e^{*2}\lambda^8 - 2\xi_1\left(\lambda^2\mathrm{Cos}^2\alpha + \lambda^2\mathrm{Sin}^2\alpha - 1\right)\lambda^{-4}\mathrm{Cos}^2\alpha - \lambda^{-6} + 1 = 0. \tag{13}$$

In the simple setting of homogeneous equibiaxial deformation, the stability criterion in order to obtain the taut domains is expressed as

$$\frac{dS^*(\lambda, \lambda)}{d\lambda} > 0. \tag{14}$$

In the forthcoming section, the governing equation (11) is solved numerically to obtain the taut domains for a proposed transversely isotropic electroactive material-based smart thin membrane.

3 Results and discussions

In this section, the electromechanical model presented in Section 2 is utilized for predicting the thresholds on the taut domains in the plane of principal stretches by varying several input parameters. First, the analytical findings are obtained for the special case of an isotropic smart thin membrane for different levels of applied electrical loading conditions. Next, the impact of the fiber strength and its orientations in principal directions on the taut domains under electric field loading conditions are examined. To examine the effect of fiber reinforcement, five different values of anisotropy parameter $\xi_1 = 0, 0.05, 0.10, 0.15, 0.20$ [27] are adopted. The anisotropy parameter accounting for the shear coupling effect is neglected, i.e., $\xi_2 = 0$ in this study. Further, the value of $\alpha = 0°, 30°, 45°, 60°, 90°$ [27] are considered to analyze the effect of fiber-orientation.

3.1 Taut domains of isotropic smart thin membrane

In this subsection, first we investigate our constructed model (11) in the absence of anisotropy effect. For a given $\xi_1 = 0$, our model represents the dielectric elastomer membrane characteristics actuated by varying electric field (e^*). In order to investigate the taut domain obtained from the developed model with $\xi_1 = 0$, the obtained principal stretches (λ_1 and λ_2) are plotted in Fig. 3. The obtained critical electrical field $e^*_{crit.} = 0.687$ at which taut domain reduces to a point represents the onset of pull-in instability and matches well with the prior investigations [28, 29]. The developed theoretical model captures the trend of variation of the taut domains in the plane of principal stretches (λ_1 and λ_2) with the applied electric field. Further, an exact one-to-one corroboration in taut domains for an applied level of an electric field is observed

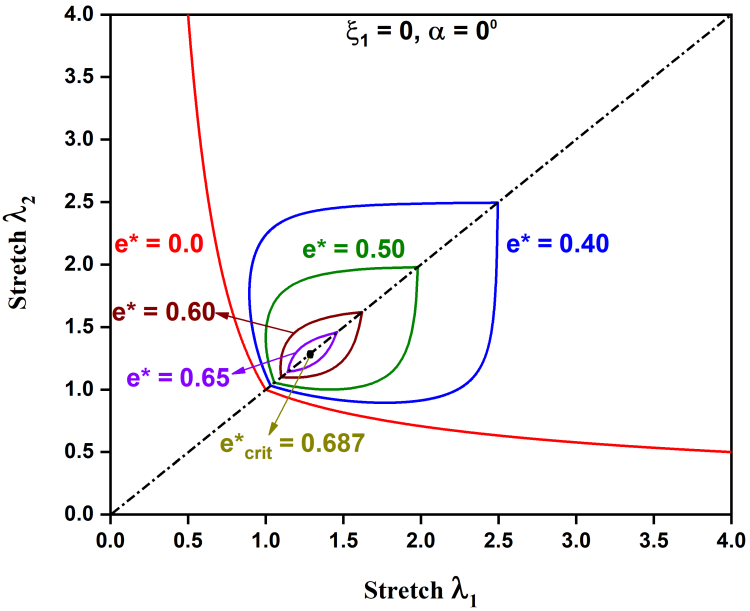

Figure 3: Taut domains of isotropic ($\xi_1 = 0$) smart thin membrane for varying level of applied electric field.

between the DeTommasi et al. [17] model and the developed model. This observation ascertains the legitimacy of the developed model in accurately predicting the taut domains in the plane of principal stretches.

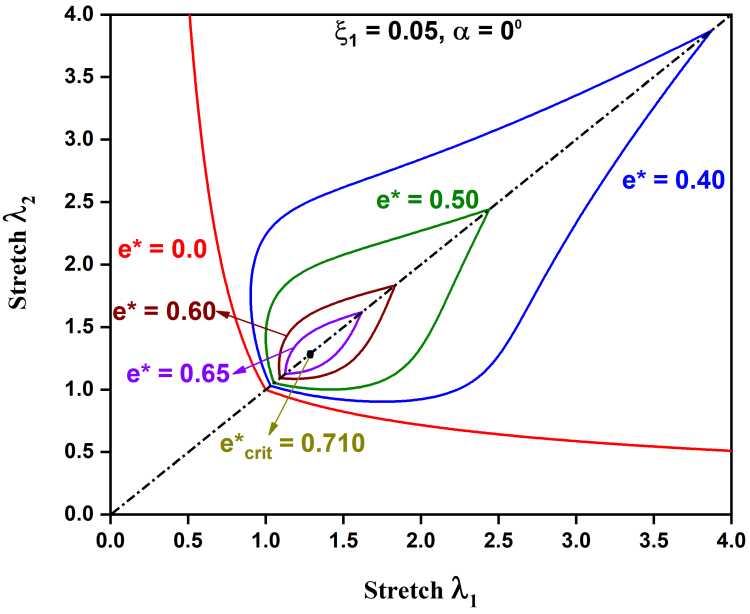

Figure 4: Taut domains of transversely isotropic smart membrane for varying electric field e^*.

3.2 Taut domains in transversely isotropic smart thin membrane in presence of electric field

This subsection investigates the taut domains of transversely isotropic thin membrane subjected to electric loading conditions. The electroactive thin membrane with anisotropy parameter $\xi_1 = 0.05$ and fiber orientation $\alpha = 0°$ is considered. First, the taut domain of the membrane for varying electric field levels is obtained as revealed in Fig. 4. The taut region shrinks as e^* is increased, i.e., as the voltage rises, until a critical activation $e^*_{crit.}$ is reached. The taut domain of transversely isotropic membrane reduces to a point for $e^*_{crit.} = 0.710$. There are no taut states at higher voltages. It is worth noting that a higher e^* correlates to a lower elastic modulus μ. As a result, it can be deduced that stiffer materials have a greater tensile stretch region [17].

3.3 Effect of fiber reinforcement and orientation on the taut domain

In the following subsection, the effect of fiber reinforcement and its orientation on the taut states of transversely isotropic thin membrane activated by electric loading is studied. In the first case, we analyze the effect of fiber reinforcement for the five aforementioned sets of anisotropy parameter ξ_1 with $\alpha = 0°$, $e^* = 0.70$(see Fig. 5a). From Fig. 5a, it is clearly observed that the taut domains for a particular level of applied electric field increase with an increase in the anisotropy parameter. This implies that the fiber reinforcement resists or even suppresses the wrinkling [27] (obtained outside the taut domain, see Fig. 2). This positive impact of fiber re-

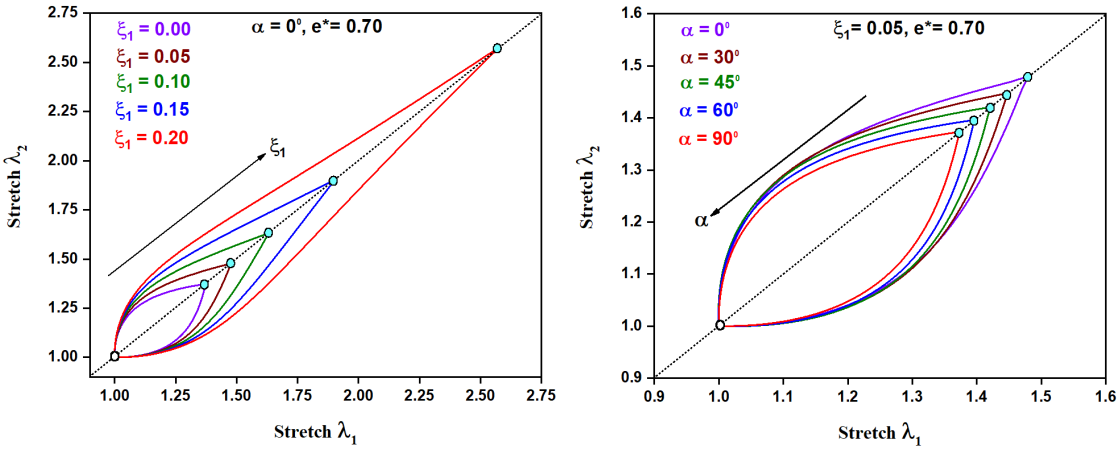

(a) (b)

Figure 5: Taut domains of a transversely isotropic smart membrane for (a) varying anisotropy parameter ξ_1 at $\alpha = 0°$, and (b) varying fiber orientation angle α at $\xi_1 = 0.05$, excited by electric loading conditions of $e^* = 0.70$.

inforcement provides a promising design technique for wrinkle-resistant or wrinkle-free surfaces. In the second case, we investigate the effect of fiber orientation for different aforementioned values of α with $\xi_1 = 0.05$, $e^* = 0.70$ (see Fig. 5b). It is observed from Fig. 5b that for an applied electric field, the domain of the taut state depleted with an enhancement in the fiber orientation. This implies that the thin membrane with oriented fiber ($\alpha > 0°$) is more susceptible to wrinkling phenomenon in comparison to the membrane without orientation ($\alpha = 0°$).

4 CONCLUSIONS

The current research proposes a continuum mechanics-based model for predicting the taut domain thresholds of a transversely isotropic electroactive thin membrane class. The notion of natural width under simple tension is used to create the coupled nonlinear equation that evaluates the taut domains. The taut domains of transversely isotropic thin membranes depleted with an increase in the applied level of electrical loading. On parallel lines, for an applied electrical loading, the taut domains of transversely isotropic thin membranes amplifies with an enrichment in the anisotropy parameter; whereas it depleted with an increase in the fiber orientations from 0^0 to 90^0. Hence, it is observed that the extent of taut domains of transversely isotropic thin membranes can be controlled by modifying the level and the principal direction of the transverse isotropy.

Finally, the inferences of this work may aid in the development of wrinkle-tunable fiber-reinforced surfaces for smart devices.

Acknowledgment

The authors are grateful for the financial support provided by the Indian Institute of Technology Roorkee, India.

REFERENCES

[1] Kumar D, Ghosh S, Roy S, Santapuri S. Modeling and analysis of an electro-pneumatic braided muscle actuator. Journal of Intelligent Material Systems and Structures. (2021);32(4):399-409.

[2] Biddiss E, Chau T. Dielectric elastomers as actuators for upper limb prosthetics: Challenges and opportunities. Medical engineering and physics. (2008);30(4):403-18.

[3] Khurana A, Kumar A, Raut SK, Sharma AK, Joglekar MM. Effect of viscoelasticity on the nonlinear dynamic behavior of dielectric elastomer minimum energy structures. International Journal of Solids and Structures. (2021);208:141-53.

[4] Khurana A, Sharma AK, Joglekar MM. Nonlinear oscillations of electrically driven aniso-visco-hyperelastic dielectric elastomer minimum energy structures. Nonlinear Dynamics. (2021) May;104(3):1991-2013.

[5] Sharma AK, Bajpayee S, Joglekar DM, Joglekar MM. Dynamic instability of dielectric elastomer actuators subjected to unequal biaxial prestress. Smart Materials and Structures. (2017);26(11):115019.

[6] Gangwar A.S., Agrawal Y., and Joglekar D.M. Nonlinear interactions of lamb waves with a delamination in composite laminates. Journal of Nondestructive Evaluation, Diagnostics and Prognostics of Engineering Systems. (2021);4(3).

[7] Gour S., Kumar D. and Khurana A. Constitutive modeling for the tear fracture of artificial tissues in human-like soft robots. European Journal of Mechanics-A/Solids. (2022); p.104672.

[8] Agrawal Y., Gangwar A.S. and Joglekar D.M. Dynamic Mixing of lamb waves at delamination defect in a unidirectional gfrp laminate. Advances in Non-destructive Evaluation. (2021);317–328.

[9] Agrawal Y., Gangwar A.S. and Joglekar D.M. Localization of a Breathing Delamination Using Nonlinear Lamb Wave Mixing. Journal of Nondestructive Evaluation, Diagnostics and Prognostics of Engineering Systems. (2022);5(3), p.031005.

[10] Khurana A., Joglekar M.M. and Zurlo G. Electromechanical stability of wrinkled dielectric elastomers. International Journal of Solids and Structures.(2022);246, p.111613.

[11] Kumar A., Khurana A., Sharma A.K. and Joglekar M.M. Dynamics of pneumatically coupled visco-hyperelastic dielectric elastomer actuators: Theoretical modeling and experimental investigation. European Journal of Mechanics-A/Solids.(2022); 95, p.104636.

[12] Khurana A., Kumar A., Sharma A.K. and Joglekar M.M. Effect of polymer chains entanglements, crosslinks and finite extensibility on the nonlinear dynamic oscillations of dielectric viscoelastomer actuators. Nonlinear Dynamics.(2021); pp.1227-1251.

[13] Sharma A.K., Khurana A. and Joglekar M.M.A finite element model for investigating the thermo-electro-mechanical response of inhomogeneously deforming dielectric elastomer actuators. European Journal of Computational Mechanics.(2021); pp.387-408.

[14] Khurana A., Patra A.K., Joglekar M.M. An energy-based model of dielectric elastomer minimum energy structures with stiffeners: Equilibrium configuration and the electromechanical response. Mechanics of Advanced Materials and Structures.(2022); 18:1-9.

[15] De Tommasi D, Puglisi G, Zurlo G. Compression-induced failure of electroactive polymeric thin films. Applied Physics Letters. (2011);98(12):123507.

[16] He T, Zhao X, Suo Z. Dielectric elastomer membranes undergoing inhomogeneous deformation. Journal of Applied Physics. (2009);106(8):083522.

[17] De Tommasi D, Puglisi G, Zurlo G. Taut states of dielectric elastomer membranes. International Journal of Non-Linear Mechanics. ()2012);47(2):355-61.

[18] Li K, Wu W, Jiang Z, Cai S. Voltage-induced wrinkling in a constrained annular dielectric elastomer film. Journal of Applied Mechanics. (2018);85(1):011007.

[19] Shui L, Liu Y, Li B, Zou C, Tang C, Zhu L, Chen X. Mechanisms of electromechanical wrinkling for highly stretched substrate-free dielectric elastic membrane. Journal of the Mechanics and Physics of Solids. (2019);122:520-37.

[20] Sharma AK, Arora N, Joglekar MM. DC dynamic pull-in instability of a dielectric elastomer balloon: an energy-based approach. Proceedings of the Royal Society A: Mathematical, Physical and Engineering Sciences. (2018);474(2211):20170900.

[21] Rudykh S., Bhattacharya K., Debotton G. Snap-through actuation of thick-wall electroactive balloons. International Journal of Non-Linear Mechanics. (2012);47(2):206-9.

[22] Zhang J, Chen H, Li D. Pinnacle elimination and stability analyses in nonlinear oscillation of soft dielectric elastomer slide actuators. Nonlinear Dynamics. (2018);94(3):1907-20.

[23] Sharma A.K., Joglekar M.M. Effect of anisotropy on the dynamic electromechanical instability of a dielectric elastomer actuator. Smart Materials and Structures. (2018);28(1):015006.

[24] Kumar D., Sarangi S. Electro-magnetostriction under large deformation: modeling with experimental validation. Mechanics of Materials.(2019);128:1-0.

[25] Steigmann DJ, Pipkin AC. Finite deformations of wrinkled membranes. The Quarterly Journal of Mechanics and Applied Mathematics. (1989);42(3):427-40.

[26] Bustamante R. Transversely isotropic non-linear electro-active elastomers. Acta mechanica. (2009);206(3):237-59.

[27] Yang Y, Fu C, Xu F. A finite strain model predicts oblique wrinkles in stretched anisotropic films. International Journal of Engineering Science. (2020);155:103354.

[28] Sharma A.K., Bajpayee S, Joglekar D.M., Joglekar M.M. Dynamic instability of dielectric elastomer actuators subjected to unequal biaxial prestress. Smart Materials and Structures. (2017);26(11):115019.

[29] Joglekar M.M. An energy-based approach to extract the dynamic instability parameters of dielectric elastomer actuators. Journal of Applied Mechanics.;81(9).

[30] De Tommasi D, Puglisi G, Zurlo G. Failure modes in electroactive polymer thin films with elastic electrodes. Journal of Physics D: Applied Physics. (2014);47(6):065502.

[31] Kofod G. The static actuation of dielectric elastomer actuators: how does pre-stretch improve actuation?. Journal of Physics D: Applied Physics. (2008);41(21):215405.